



Recovery of organic matters in wastewater by self-forming dynamic membrane bioreactor: Performance and membrane fouling

Ling Wang^a, Hongbo Liu^{a, b, **}, Wenduo Zhang^a, Tiantian Yu^a, Qiu Jin^a, Bo Fu^{a, b}, He Liu^{a, b, *}

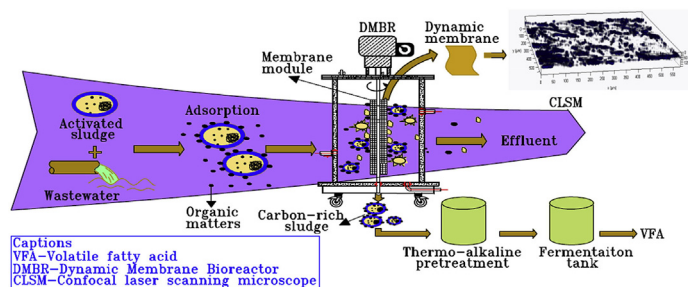
^a Jiangsu Key Laboratory of Anaerobic Biotechnology, School of Environmental and Civil Engineering, Jiangnan University, Wuxi 214122, PR China

^b Jiangsu Collaborative Innovation Center of Technology and Material of Water Treatment, Suzhou 215011, PR China

HIGHLIGHTS

- A novel SF-DMBR system was developed to quickly recover organics in wastewater.
- Recovery rate of carbon source in wastewater reached as high as 80%.
- High membrane fluxes were realized.
- Less protein content contributed to the weaker membrane fouling.
- The evolutions of the fouling components were determined by CLSM.

GRAPHICAL ABSTRACT



ARTICLE INFO

Article history:

Received 19 September 2017

Received in revised form

22 March 2018

Accepted 26 March 2018

Available online 26 March 2018

Handling Editor: Chang-Ping Yu

Keywords:

Carbon source recovery

Sludge adsorption

Self-forming dynamic membrane bioreactor

Membrane fouling

ABSTRACT

Formation process and fouling characteristics of the dynamic membrane were studied in a modified self-forming dynamic membrane bioreactor (SF-DMBR) for recovering the organic matters in wastewater, and the performance of this SF-DMBR was investigated. Results indicated that 80% of the organic matters in wastewater could be quickly recovered under continuous operation. Furthermore, the evolutions of the fouling components were determined during the formation and development processes of dynamic membrane. After the long-term operation, the decreases of protein concentration, accompanying with the increases of polysaccharides and microorganisms contents due to special operating conditions, were interestingly observed in the sludge of membrane surface. This could explain why membrane fouling was much weak. Therefore, though high membrane fluxes at 50–150 L/(m²·h) were adopted in this study, the reactor can still obtain a long-term stable operation and the operating cycle reached as long as 8 days. Finally, membrane fouling process was described by combined models.

© 2018 Elsevier Ltd. All rights reserved.

1. Introduction

In the 1960s, the new concept of “21st century water plant” has

been proposed and already attracted wide attentions for its potential application. Compared with conventional wastewater treatment process, it tends to recover the organic matters in

* Corresponding author. Jiangsu Key Laboratory of Anaerobic Biotechnology, School of Environmental and Civil Engineering, Jiangnan University, Wuxi 214122, PR China.

** Corresponding author. Jiangsu Key Laboratory of Anaerobic Biotechnology, School of Environmental and Civil Engineering, Jiangnan University, Wuxi 214122, PR China.

E-mail addresses: liuhongbo@jiangnan.edu.cn (H. Liu), liuhe@jiangnan.edu.cn (H. Liu).

wastewater rather than simply removes it or converts it into no value-added products (such as carbon dioxide, nitrogen, waste phosphate, etc.) (Ansari et al., 2016; Gong et al., 2017), reducing energy consumption and avoiding generation of excess sludge (Mccarty et al., 2011). Therefore, it is meaningful to develop technologies for recovering low value-added organic matters from wastewater.

Concentrating and enrichment are the premises to achieve the resource utilization of those organic matters in urban wastewater. There are already a few methods for concentrating organic matters in urban wastewater, including coagulation (Akanyeti et al., 2010; Frijns et al., 2013), forward osmosis process (Alturki et al., 2013; Cath et al., 2013; Lutchmiah et al., 2014), membrane separation (Bourgeois et al., 2001; Cai, 1999) and adsorption (Kartal et al., 2010), etc. Lutchmiah et al. (2011) recovered high-quality water by means of forward osmosis (FO), and the subsequent concentrated sewage (containing an inherent energy content) can be converted into a renewable energy. Akanyeti et al. (2010) recovered at least 35% of the sewage COD by bioflocculation. However, all of those technologies were seriously hindered by the high operation cost.

SF-DMBR is a promising sewage treatment technology, in which the dynamic membrane is actually a fouling layer forming on inexpensive support materials with relative big pores (such as non-woven fabrics, sieves, etc.). It shows the advantages of high membrane fluxes, high retention rate of substrates, low energy consumption and low operation costs (Chu et al., 2010). Moreover, it is known that the reaction between microorganisms and organic matters could be divided into two stages (Guellil et al., 2001; Gao et al., 2007), adsorption and degradation, in wastewater treatment processes. Therefore, if the hydraulic retention time (HRT) of SF-DMBR was kept short enough, the adsorption process would dominate while microbial metabolism would be in a position of weakness, and finally organic matters in wastewater could be concentrated. Based on the above-mentioned descriptions, a modified SF-DMBR was built and operated with short HRT and high membrane fluxes.

Membrane fouling might be the key factor hindering the operation of this modified SF-DMBR, though it presents great potential in concentrating and recovery of organic matters from wastewater (Gong et al., 2014). There are many factors influencing membrane fouling, such as configuration of membrane module (Xiong et al., 2014), aeration strength (Kiso et al., 2000), membrane flux (Fuchs et al., 2005; Ren et al., 2010) and characteristics of the separating substrates (Hu et al., 2017), etc. Obviously, comparing with common SF-DMBRs for wastewater treatment, the modified SF-DMBR for organic matters recovery has to be operated under high membrane fluxes and different separating substrates. Firstly, high membrane flux could provide short HRT, but also would result in terrible membrane fouling. Then, the primary sludge is the separating substrate of the modified SF-DMBR and has different characteristics from the secondary sludge, such as low proteins content, good dewaterability, which thus would relieve membrane fouling. Therefore, the feasibility of this modified SF-DMBR should be studied and evaluated for organic matters recovery from wastewater.

In this study, the formation process and fouling characteristics of the dynamic membrane were studied in the modified SF-DMBR for recovering organic matters from wastewater. The main objectives of this study are: (1) to evaluate the performance of the modified SF-DMBR in recovering organic matters from wastewater, (2) to analyze the operation stability of dynamic membrane, (3) to study the characteristics of the membrane fouling under high fluxes and (4) to investigate the mechanism of membrane fouling.

2. Materials and methods

2.1. Wastewater

Samples of urban wastewater used in this study were synthetic wastewater and the components were reported in the previous literature (Chu et al., 2014). Water quality indexes were shown in the following Table 1. Activated sludge was collected from the aeration tank of the wastewater treatment plant in Wuxi city, China. Considering that starvation phase plays an essential role on the adhesion process, activated sludge need to be aerated without feed before used in order to obtain the better adsorption (Li et al., 2006).

2.2. SF-DMBR and experimental set-up

The schematic diagram of the experimental set-up was shown in Fig. 1. The dynamic membrane bioreactor was the main body with a working volume of 14 L, which mainly consisted of a stirrer and a membrane module. The support material of the dynamic membrane was woven-fabric mesh with pore size of 150 μm and membrane area of 0.04 m^2 . A polyamide nylon mesh wound over a hollow cylindrical support made of the polyvinyl chloride with an external diameter of 51 mm and an internal diameter of 21 mm and a length of 140 mm. When the flux was changed, the support membrane was replaced. In the reactor, the stirring device was used instead of the aeration equipment, which was fixed together with the membrane module at a rotating speed of 35 r/min, it can provide a suitable cross flow in addition to mixing. The bioreactor was operating in a anaerobic condition with temperature 25 $^{\circ}\text{C}$ and pH 7.0.

The reactor was equipped with a feed tank, a peristaltic pump and an effluent tank. Activated sludge with a concentration of

Table 1
Water quality index.

Water quality index	Values
SCOD ($\text{mg}\cdot\text{L}^{-1}$)	250 \pm 25
TSS ($\text{mg}\cdot\text{L}^{-1}$)	3000 \pm 44
TN ($\text{mg}\cdot\text{L}^{-1}$)	25 \pm 0.8
TP ($\text{mg}\cdot\text{L}^{-1}$)	7.9 \pm 0.8

Values are given as mean values \pm standard deviation.

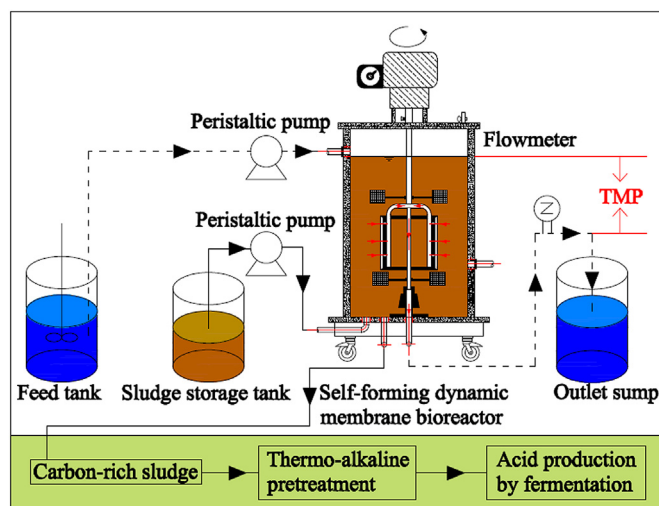


Fig. 1. The schematic diagram of the experimental set-up.

Table 2
Summary of the five constant flow combined fouling models.

Models	Component mechanisms	Equation	Fitted parameters
Cake-complete	Cake filtration, complete blocking	$\frac{P}{P_0} = \frac{1}{(1-K_b t)} \left(1 - \frac{K_c J_0^2}{K_b} \ln(1 - K_b t) \right)$	$K_c(\text{s/m}^2)$, $K_b(\text{s}^{-1})$
Cake-intermediate	Cake filtration, intermediate blocking	$\frac{P}{P_0} = \exp(K_i J_0 t) \left(1 + \frac{K_c J_0}{K_i} (\exp(K_i J_0 t) - 1) \right)$	$K_c(\text{s/m}^2)$, $K_i(\text{m}^{-1})$
Complete-standard	Complete blocking, standard blocking	$\frac{P}{P_0} = \frac{1}{(1-K_b t) \left(1 + \frac{K_s J_0}{2K_b} \ln(1-K_b t) \right)^2}$	$K_b(\text{s}^{-1})$, $K_s(\text{m}^{-1})$
Intermediate-standard	Intermediate blocking, standard blocking	$\frac{P}{P_0} = \frac{\exp(K_i J_0 t)}{\left(1 - \frac{K_s}{2K_i} (\exp(K_i J_0 t) - 1) \right)^2}$	$K_i(\text{m}^{-1})$, $K_s(\text{m}^{-1})$
Cake-standard	Cake filtration, standard blocking	$\frac{P}{P_0} = \left(\left(1 - \frac{K_s J_0 t}{2} \right)^{-2} + K_c J_0^2 t \right)$	$K_c(\text{s/m}^2)$, $K_s(\text{m}^{-1})$

J-flux (m/s); J_0 -initial flux (m/s); K_b -complete blocking constant (s^{-1}); K_c -cake filtration constant (s/m^2); K_i -intermediate blocking constant (m^{-1}); K_s -standard blocking constant (m^{-1}); P- pressure (kg/ms^2); P_0 - initial pressure (kg/ms^2).

3000 mg/L flowed into the reaction chamber through the sludge pipe in the bottom, while the wastewater was pumped into the reactor by a peristaltic pump. The concentration of sludge (in the form of TSS) in the reactor was measured once a day and maintained at 3000 mg/L through discharging sludge regularly. The reactor was started up when the liquid level reached the level at setting value. Organic matters were concentrated in the sludge because they were quickly adsorbed by activated sludge in a short period. This period was set as HRT for 50 min. Meanwhile, the activated sludge deposited on the nylon mesh, thus the dynamic membrane gradually formed. The effluent was discharged with gravity, while the sludge was trapped in the reactor by membrane. The activated sludge in the reactor was subjected to recover after saturation for subsequent acid production by fermentation after thermo-alkaline pretreatment.

The study was conducted with different high fluxes to investigate the removal of organic matters and the stability of the reactor. The membrane fluxes adopted in this study were larger than the majority of existing literatures, which were 50, 100, 150 L/($\text{m}^2 \cdot \text{h}$), respectively. In this test, a silicone hose was used to connect to the water collecting pipe. Therefore, the flux could be controlled constantly at set value by adjusting the height of whose outlet.

2.3. Confocal laser scanning microscopy (CLSM)

The fouled membrane that was taken out from the reactor operated with a membrane flux of 100 L/($\text{m}^2 \cdot \text{h}$) was studied to investigate the growth of cake layer with CLSM. According to the change of the membrane resistance, the membrane samples were carried out when the SF-DMBR was operated for hours 26, 113 and 140, respectively.

The staining materials used in this study were Concanavalin A (ConA) purchased from Molecular Probes, Calcofluor white (CW) purchased from Sigma, Fluorescein isothiocyanate (FITC) purchased from Molecular Probes and SYTO 63 purchased from Molecular Probes (Yang et al., 2007). Every membrane sample was cut into a size of about 0.5 cm \times 0.5 cm. Firstly, SYTO 63 (20 μM) used to label the microorganisms was dipped on the fouled membrane sample, placing on a shaker table for 30 min. Secondly, 1 M sodium bicarbonate buffer was added to maintain the amine group in non-protonated form. Next, the sample was stained with the FITC solution (10 g/L) at room temperature for labelling the proteins. Then, the ConA solution (0.25 g/L) was added to the sample for labelling α -D-glucopyranose polysaccharides. Subsequently, Calcofluor white (0.3 g/L) was adopted to stain the β -D-glucopyranose polysaccharides. After each stage of the labeling process, the sample was incubated for 30 min at room temperature in the dark, and then was washed twice with phosphate buffered saline (PBS)

solution to remove the extra probes. Every step must be done in the dark.

Confocal laser scanning microscopy (CLSM; ZEISS LSM 710, ZEISS, Germany) was used to characterize the stained membrane samples. The CLSM images were generated in multi track mode, and excitation and emission wavelengths of each dye were adopted according to the methods described by Yuan et al. (2015).

2.4. Hydrophilicity

Contact angle on the membrane surface was measured by sessile drop method with the Data-Physics OCA15 contact angle analyzer (DataPhysics Instruments GmbH, Filderstadt, Germany). The droplet (deionized water) with volume of 1 μL and with a rate of 1 L/s formed on the membrane surface at room temperature. The injection speed was 5 $\mu\text{L s}^{-1}$. A side-view picture was captured after 10 s. Each measurement was made in triplicate and the average of three measurements was calculated (Zou et al., 2011).

2.5. Combined models of membrane fouling

According to the methods described by Bolton et al. (2006), changes of resistance may be caused by multiple reasons, so it is meaningful to combine the single models. Therefore, based on the method in the literature, we carried out the fitting of the resistance data under continuous feeding conditions. The models adopted were shown in the following Table 2 (Bolton et al., 2006).

2.6. Analytical methods

Samples were collected in influent and effluent. Conventional indexes, including chemical oxygen demand (COD), total suspended solids (TSS), total nitrogen (TN) and total phosphorus (TP) were analyzed according to the standard methods issued by the State Environmental Protection Administration of China (2002). Soluble carbohydrates were measured by the phenol-sulfuric method with glucose as standard (Dubois et al., 1956). Soluble proteins were determined by the Lowry-Folin method with bovine serum albumin (BSA) as standard (Lowry et al., 1951). The different extracellular polymeric substances (EPS) layers, including loosely bound extracellular polymeric substances (LB-EPS) and tightly bound extracellular polymeric substances (TB-EPS), were extracted by centrifugation and ultrasound method (Yuan et al., 2017). The filtration resistance was calculated using the following equation:

$$R = \frac{TMP}{\mu J} \quad (1)$$

where R is the total membrane resistance (m^{-1}), J is the instantaneous flux ($m^3 \cdot m^{-2} \cdot h^{-1}$), μ is the dynamic viscosity of permeate water ($Pa \cdot s$) (Zhang et al., 2010).

3. Results and discussion

3.1. Performance of modified SF-DMBR in organic matters recovery from wastewater

High recovery efficiency of organic matters was observed in SF-DMBR from wastewater. As shown in Fig. 2, though very high membrane fluxes were adopted, the concentrations of all substrates in effluent, namely SCOD, TN and TP, could quickly drop at first and then stabilize at very low levels. The recovery rates of COD, TN and TP were up to about 80%, 10% and 30%, respectively. As shown from the results, 80% of organic matters can be recovered. However, compared with the results of other literature in the DMBRs, the recovery rates of TN and TP were relatively low (Chu et al., 2014). Perhaps it is because the nitrogen and phosphorus in the synthetic wastewater are soluble, while the adsorption of the activated sludge for the small soluble molecules is relatively weak.

3.2. Contributions of the dynamic membrane separation on organic matters recovery

Dynamic membrane presents high efficiency in liquid-solid separation. The rejection effect of total suspended solids (TSS) by dynamic membrane was shown in Fig. 3. It can be seen that the concentration of TSS in the effluent firstly decreased and then kept stable. The dynamic membrane had not yet formed at the start of the reactor, the interception capacity of TSS was relatively low throughout this period. However, a good particle rejection was

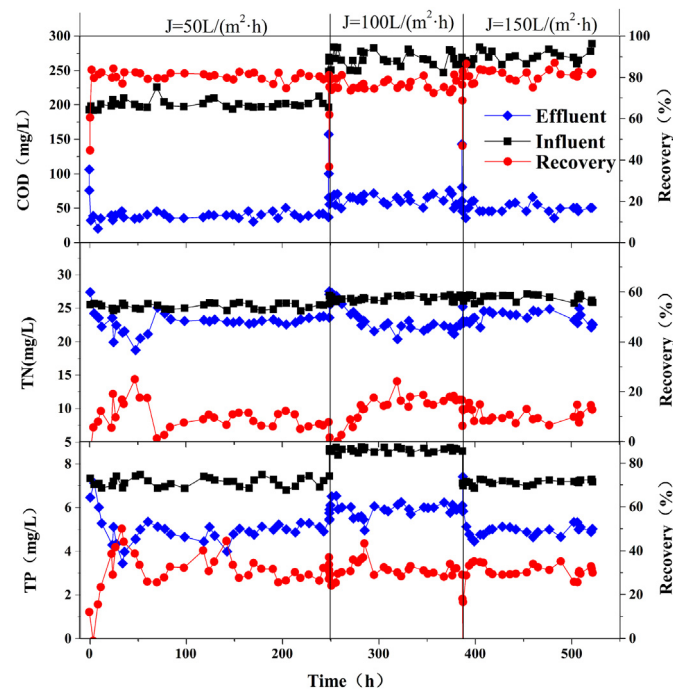


Fig. 2. Recovery of organic matters in wastewater.

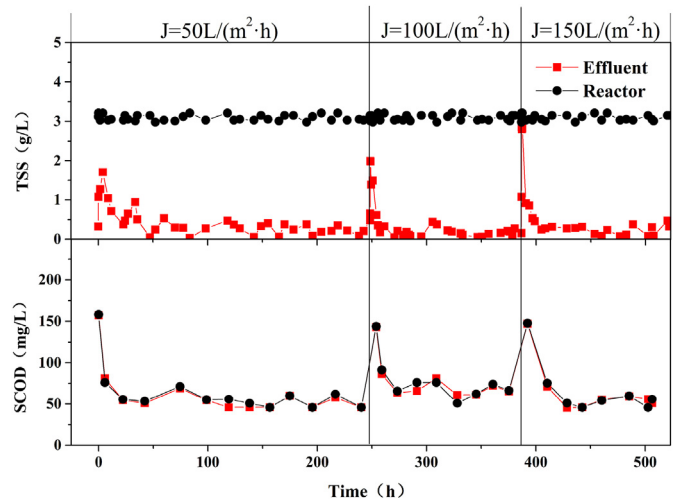


Fig. 3. The changes of TSS and SCOD in reactor and effluent.

quickly obtained after the formation of dynamic membrane within 20 h, and TSS concentration in the effluent was maintained at a low and stable level. However, the SCOD concentrations in the reactor and in effluent did not show significant differences, indicating that the action of the DM was mainly to trap suspended solids which adsorbed organic matters from wastewater. Because urban wastewater used in this study were synthetic wastewater, suspended solids in influent were negligible. This means that the contribution of DM to recovery of organic matters was mainly reflected in retention to activated sludge that adsorbed organics. The loss of adsorbed organic matters, to a great extent, was avoided through the high efficient solid-liquid separation. Therefore, the recovery rate of organic matters was improved indirectly by the DM.

Moreover, the low turbidity in effluent means the formation of the DM (Xiong et al., 2014). According to the retention efficiency of TSS, the formation time was diverse under different fluxes. When the membrane flux was at a relatively low level of about 50 L/($m^2 \cdot h$), the concentration of TSS in the effluent tended to stabilize after 20 h, much higher than 10 and 9 h corresponding to the fluxes of 100 and 150 L/($m^2 \cdot h$), respectively, suggesting the faster formation of the DM under higher fluxes.

3.3. Membrane fouling of SF-DMBR under high membrane fluxes

Membrane fouling developed slowly though high membrane fluxes were adopted in this study. The changes of membrane resistance under different membrane fluxes were shown in Fig. 4A. In most of the previous literatures, the reactors often run under relatively small membrane fluxes of around 20 L/($m^2 \cdot h$) (Duan et al., 2011; Ersahin et al., 2012; Ren et al., 2010; Zhou et al., 2008). In this study, the SF-DMBR could operate steadily for a long period of more than 5 days though the membrane flux reached as high as 150 L/($m^2 \cdot h$). This good performance should be attributed to many factors except for the supported materials with large pore size, such as the nature of the sludge, mixing method and so on (Sun et al., 2014).

Therefore, a separate study of the reactor was conducted under the condition of 100 L/($m^2 \cdot h$). As shown in Fig. 4B, the process could be divided into three stages. The resistance declined gradually in the first stage, so the change rate of the resistance was negative. In this stage, the water contact angle of the membrane surface rapidly decreased with the formation of the DM (Fig. 4C), corresponding to a decrease in hydrophobicity (it is hydrophobic

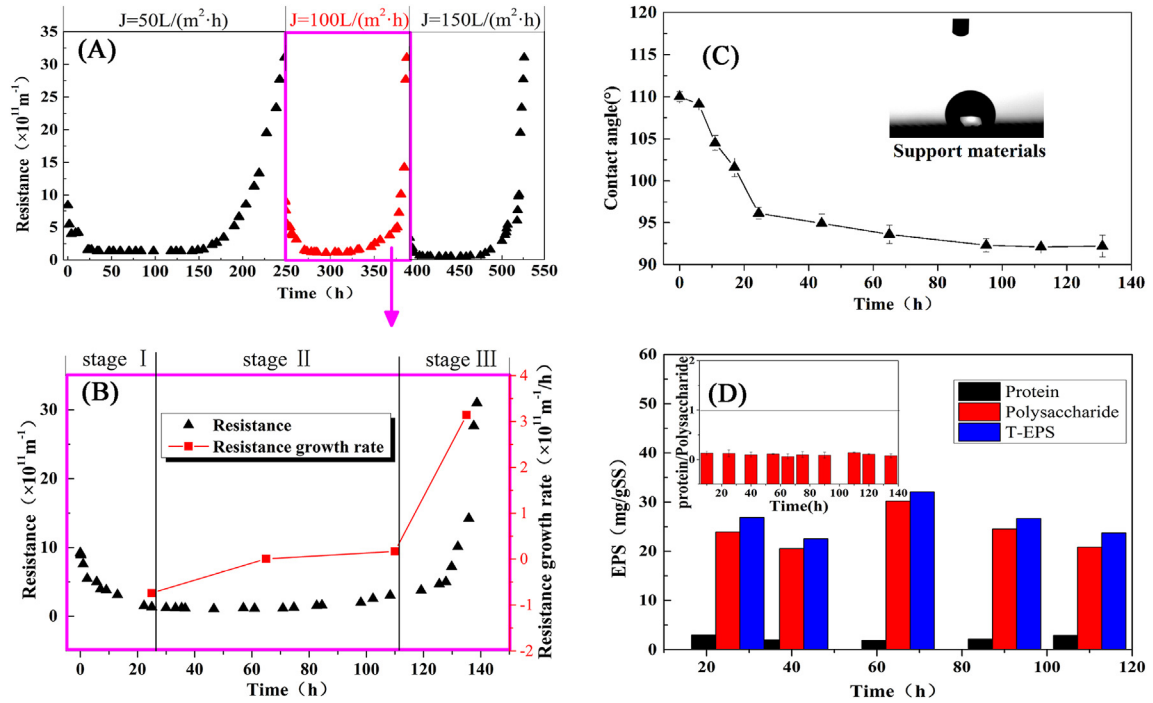


Fig. 4. Analysis of the resistance variation: (a) change of the resistance under different fluxes; (b) rate of change in resistance under the flux of $100 \text{ L}/(\text{m}^2 \cdot \text{h})$; (c) contact angle on the membrane surface; (d) the content of EPS in reactor.

when the contact angle is over 90°). The improvement of the hydrophilicity can reduce the contact and non-directional bonding between the membrane surface and the molecules intercepted,

thus reducing the amount of pollutants and sludge adsorbed on membrane surface. Therefore, the increase of hydrophilicity may be the main reason to the decrease of membrane resistance at this

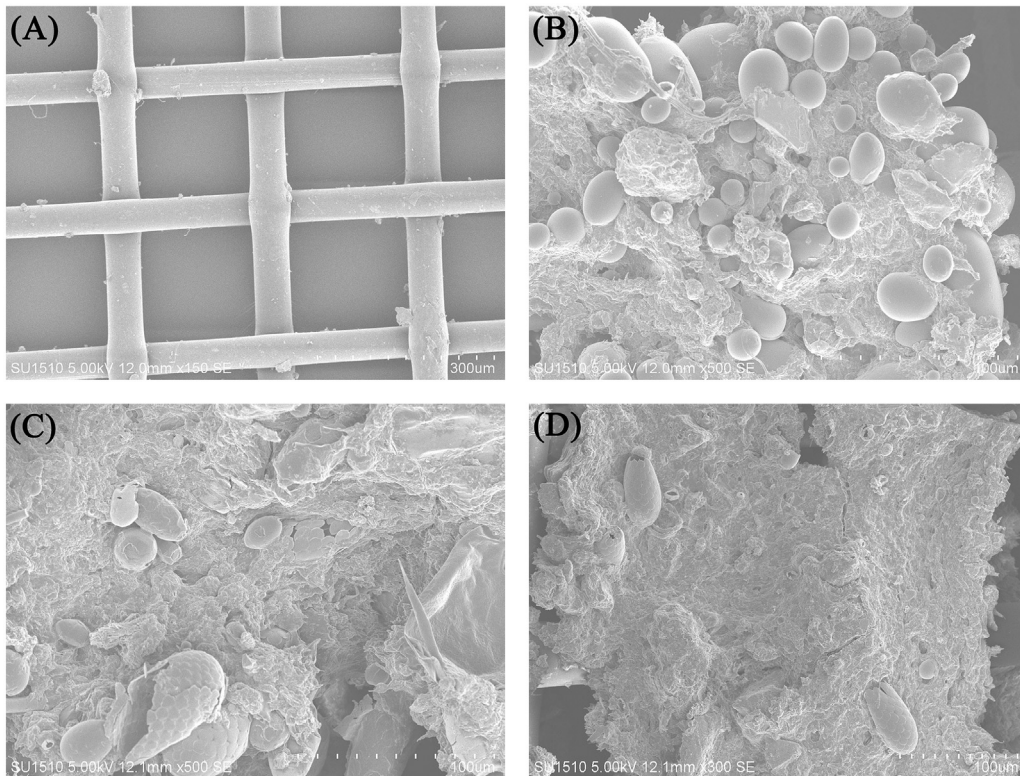


Fig. 5. SEM of membrane surface: (a) Clean membrane at $150\times$ magnification; (b) the first stage (26 h) at $500\times$ magnification; (c) the second stage (113 h) at $500\times$ magnification; (d) the third stage (140 h) at $300\times$ magnification.

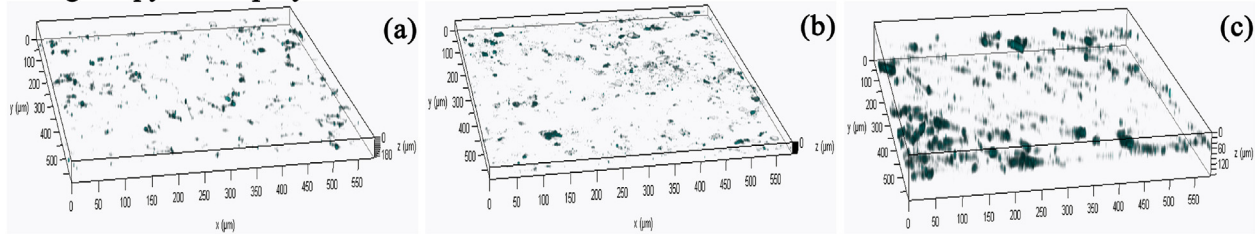
stage (Zou et al., 2011). In the second stage, the resistance tended to be stable. In other words, the increase of membrane fouling occurred slowly. At this stage, the contact angle barely changed, and the content of EPS (including polysaccharides and proteins) in the reactor was very low (Fig. 4D), especially of proteins. The ratio of proteins to polysaccharides in EPS was less than 1.0. The proteins were reported to be the main materials that cause membrane fouling (Lee et al., 2003). In the third stage, the resistance rose rapidly, which may be that the membrane holes were gradually

blocked during the operation of the reactor and the cake layer was compacted. So, the compressibility of DM was very low, which led to poor filtration performance (Vera et al., 2015).

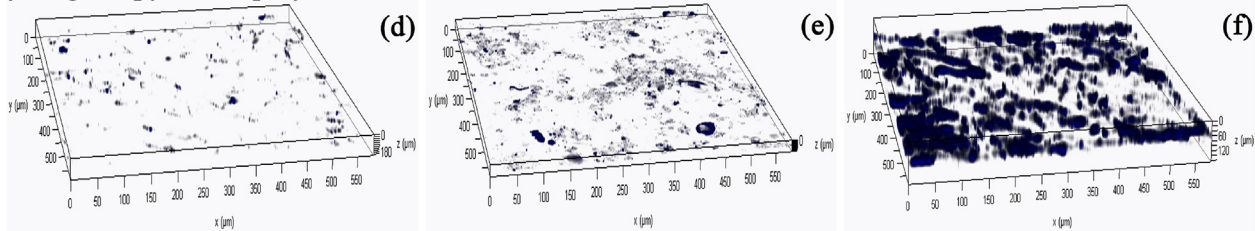
3.4. SEM observation of dynamic membrane

SEM photos of membrane surface in different stages were shown in Fig. 5. According to the methods described by Yuan et al. (2015), the changes of cake layer are divided into three stages, namely, the

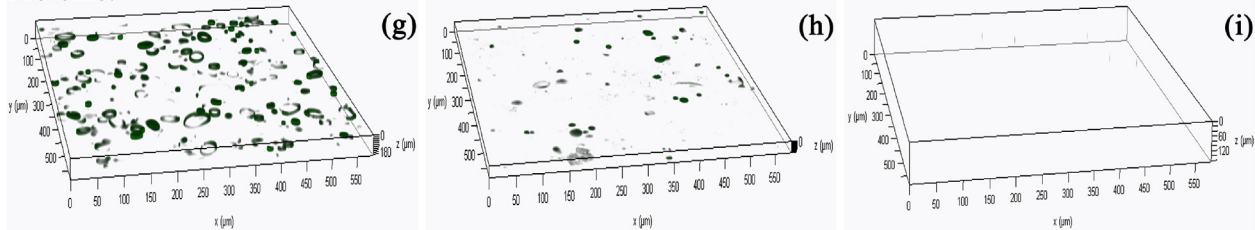
α -D-glucopyranose polysaccharides:



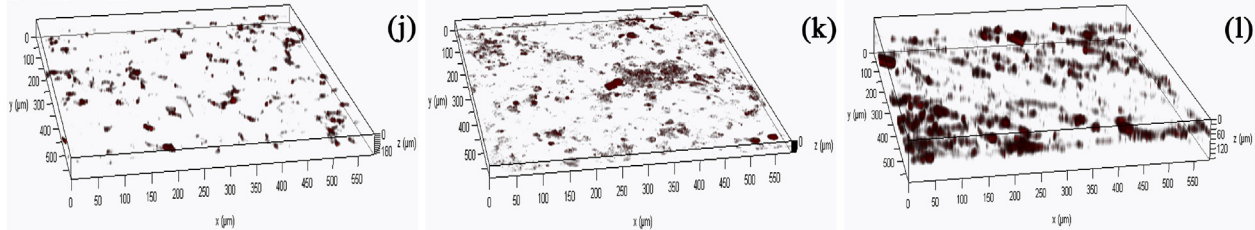
β -D-glucopyranose polysaccharides:



Proteins:



Total cells:



Integrated CLSM images:

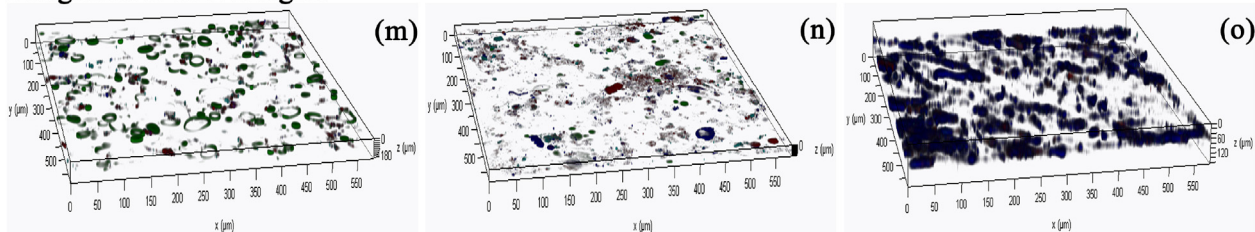


Fig. 6. CLSM images of α -D-glucopyranose polysaccharides, β -D-glucopyranose polysaccharides, proteins, total cells and Integrated images in the cake layer: (a)–(c) CLSM images of α -D-glucopyranose polysaccharides from the first stage to the third stage; (d)–(f) CLSM images of β -D-glucopyranose polysaccharides from the first stage to the third stage; (g)–(i) images of proteins from the first stage to the third stage; (j)–(l) images of total cells from the first stage to the third stage; (m)–(o) Integrated CLSM images of polysaccharides, proteins and total cells in the cake layer from the first stage to the third stage.

top cake layer, the middle cake layer and the bottom cake layer. Therefore, based on the changes of the membrane resistance, the primary pollution layer formed in the first stage, the intermediate pollution layer formed in the second stage, the top pollution layer formed in the third stage corresponding to the Section 3.3. It can be seen from the Fig. 5 that the pore size of the primary fouling layer was large and the sludge floc was relatively loose. While the pore size of the intermediate layer decreased and the sludge layer was tighter than the primary polluted layer. With the operation of the reactor, the top pollution layer was more compact.

3.5. Developing process of membrane fouling

In order to thoroughly understand the development mechanism of membrane fouling, the growth of dynamic membrane was studied by CLSM. Polysaccharides are one of the major components of biofilm (Zhang et al., 2014). Because α - and β -D-glucopyranose polysaccharides have different biodegradability and function in biological systems (Yuan et al., 2006), their changes in the DM were observed during the operation of SF-DMBR.

As shown in Fig. 6a–c, α -D-glucopyranose polysaccharides were observed on the primary fouling layer as a dot distribution. With the further growth of the cake layer, it can be observed that the amount of α -D-glucopyranose polysaccharides on the intermediate fouling layer was more than that of the primary fouling layer. At the top of the fouling layer, the distribution and abundance of α -D-glucopyranose polysaccharides developed further. However, overall, α -D-glucopyranose polysaccharides were distributed in the cluster in a highly heterogeneous manner during the operation of the reactor. It can be seen in Fig. 6d–f that β -D-glucopyranose polysaccharides were patchy deposition at the initial stage, which can be attributed to the heterogeneity and hydrodynamic conditions of membrane surface properties (Yuan et al., 2015). This initial deposition stage can help improve the properties of the membrane surface for subsequent contamination (Yuan et al., 2015). As the reactor ran, the number of β -D-glucopyranose polysaccharides on the intermediate fouling layer increased. On the top fouling layer, β -D-glucopyranose polysaccharides were thicker and denser. Compared with α -D-glucopyranose polysaccharides, β -D-glucopyranose polysaccharides were richer in the whole process. According to the literature (Chu and Li, 2005), the accumulation of polysaccharides and other biopolymers increased the fouling resistance, particularly the pore fouling resistance. Therefore, β -D-glucopyranose polysaccharides played a more important role in the growth of cake layer in this study. Polysaccharides located in the fouling layer during the OMBR operation have been proved by other literatures (Wang et al., 2014) and β -D-glucopyranose polysaccharides have also been reported to be the dominant (Yuan et al., 2015).

EPS is the main structural component of the fouling layer affecting the membrane permeability. And proteins are one of the main components of EPS (Yuan et al., 2006). It can be seen from Fig. 6g–i that the number of proteins on the primary layer was high and its distribution took on circle structure. With the operation of the reactor, the number of protein in the fouling layer was few, it was even hard to be detected on the top layer probably due to the specific operating conditions of the reactor. This result was consistent with the data of the EPS content on the DM we measured (Fig. S1). Short HRT of the reactor results in that the microorganisms in sludge do not metabolize organic matters but adsorb. Therefore, it was unable to synthesize large amounts of EPS in sludge, particularly proteins. In addition, the accumulation rate of proteins in the reactor was less than its adsorption rate. All of these reasons led to the gradual decrease of proteins on the membrane fouling layer. Previous fourier transform infrared spectroscopy (FT-

IR) studies revealed that proteins were the main materials on the fouling layer (Zhang et al., 2012), although the exact mechanism is not known. Therefore, the low content of proteins may be the main reason for the stable long-term operation of this reactor under high membrane fluxes.

The variation of the total cells was shown in Fig. 6j–l. It can be seen from the figure that, similar to the changes of β -D-glucopyranose polysaccharides, the number of cells increased gradually during the growth of the fouling layer.

In order to further evaluate the effect of EPS on the development of fouling layers, the changes in CLSM images incorporate polysaccharides, proteins and total cells were shown in Fig. 6(m–o). On the primary fouling layer, the proteins and microbial cells were the main components, that is, EPS deposited on the membrane surface, and associated with microorganisms. However, the content of proteins was much more than microorganisms from CLSM images. With the operating time, more and more β -D-glucopyranose polysaccharides deposited on the top layer, almost covering the surface and accompanied by a decrease of proteins content. Although the content of microorganisms was also increasing, its content was still less than the content of β -D-glucopyranose polysaccharides. The polysaccharides and proteins on each fouling layer had different distributions. During the growth of the fouling layer, the proteins were mainly located at the bottom and the polysaccharides were at the top, and both more than the microorganism. Therefore, in the whole process, the proteins or polysaccharides always were the main pollutants, indicating the important role of EPS in the development of fouling layer.

3.6. Combined models of membrane fouling

Fig. 7 showed the fitting models of the resistance when the membrane flux was $100 \text{ L}/(\text{m}^2 \cdot \text{h})$. In order to clarify the reason resulting in the increase of membrane resistance further, the combined models were used for the constant-flow filtration, according to the literature (Bolton et al., 2006). After fitting, it was found that the change of resistance in first stage matched with the complete-standard blocking model (as listed in Table 2). At the beginning of this stage, membrane pore size was larger than the

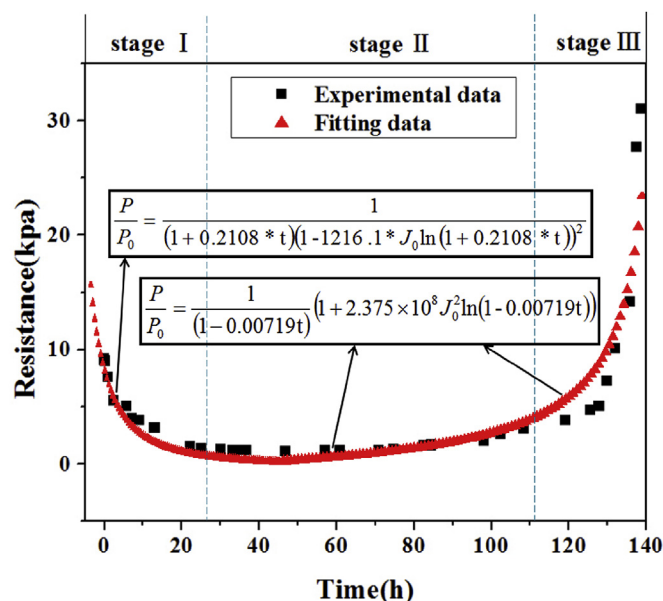


Fig. 7. Resistance vs. time data fit with the combined models.

particle size of sludge flocs, the sludge particles blocked the membrane pores and the membrane pore size decreased gradually. Afterwards, the membrane pore size was less than the particle size of sludge particles which then deposited on the membrane surface to form a single layer of sludge without gemination. The second and third stages belonged to the cake-complete clogging model, in which the sludge continued to deposit on the membrane surface, making the pore size of the membrane much smaller than the particle size. Therefore, the cake layer was compacted gradually and the compressibility was very low in this stage (Bolton et al., 2006; Vera et al., 2015), which is consistent with that described in Sections 3.3 and 3.4. Based on the above variations, the resistance increased rapidly in the third stage.

4. Conclusions

A modified SF-DMBR system was developed to recover organic matters in wastewater and the recovery efficiency of organic matters reached as high as 80%. Moreover, under high membrane fluxes of 50–150 L/(m²·h), a long-term operation of around 8 days was achieved during cross-flow filtration. Furthermore, CLSM images indicated this much weak membrane fouling in this modified SF-DMBR should contribute to the low concentration of EPS, particularly for proteins content. Finally, the complete-standard blocking model was found to be matched with the changes of membrane resistance during initial operation and cake-complete clogging model matched with that in the latter operation.

Acknowledgements

This research was financially supported by the Natural Science Foundation of Jiangsu Province of China (BK20141112), the Fundamental Research Funds for the Central Universities (JUSRP51633B), the National Key Technology R&D Program of the Ministry of Science and Technology (2014BAD24B03-02), and the Postgraduate Research & Practice Innovation Program of Jiangsu Province (SJCX17-0499).

Appendix A. Supplementary data

Supplementary data related to this article can be found at <https://doi.org/10.1016/j.chemosphere.2018.03.171>

References

- Akanyeti, I., Temmink, H., Remy, M., Zwijnenburg, A., 2010. Feasibility of bio-flocculation in a high-loaded membrane bioreactor for improved energy recovery from sewage. *Water Sci. Technol.* 61, 1433–1439.
- Alturki, A.A., McDonald, J.A., Khan, S.J., Price, W.E., Long, D.N., Elimelech, M., 2013. Removal of trace organic contaminants by the forward osmosis process. *Separ. Purif. Technol.* 103, 258–266.
- Ansari, A.J., Hai, F.I., Guo, W., Ngo, H.H., Price, W.E., Nghiem, L.D., 2016. Factors governing the pre-concentration of wastewater using forward osmosis for subsequent resource recovery. *Sci. Total Environ.* 566–567, 559–566.
- Bolton, G., Dan, L.C., Kuriyel, R., 2006. Combined models of membrane fouling: development and application to microfiltration and ultrafiltration of biological fluids. *J. Membr. Sci.* 277, 75–84.
- Bourgeois, K.N., Darby, J.L., Tchobanoglous, G., 2001. Ultrafiltration of wastewater: effects of particles, mode of operation, and backwash effectiveness. *Water Res.* 35, 77–90.
- Cai, Y., 1999. Size distribution measurements of dissolved organic carbon in natural waters using ultrafiltration technique. *Water Res.* 33, 3056–3060.
- Cath, T.Y., Elimelech, M., Mccutcheon, J.R., McGinnis, R.L., Achilli, A., Anastasio, D., Brady, A.R., Childress, A.E., Farr, I.V., Hancock, N.T., 2013. Standard methodology for evaluating membrane performance in osmotically driven membrane processes. *Desalination* 312, 31–38.
- Chu, H., Cao, D., Dong, B., Qiang, Z., 2010. Bio-diatomite dynamic membrane reactor for micro-polluted surface water treatment. *Water Res.* 44, 1573–1579.
- Chu, H., Zhang, Y., Zhou, X., Zhao, Y., Dong, B., Zhang, H., 2014. Dynamic membrane bioreactor for wastewater treatment: operation, critical flux, and dynamic membrane structure. *J. Membr. Sci.* 450, 265–271.
- Chu, H.P., Li, X.Y., 2005. Membrane fouling in a membrane bioreactor (MBR): sludge cake formation and fouling characteristics. *Biotechnol. Bioeng.* 90, 323–331.
- Duan, W., Fu, D., Zhu, Y., Xu, X., Li, C., 2011. Influence of attapulgite on biological removal characteristics of hybrid dynamic membrane reactor. *Fresenius Environ. Bull.* 20, 2943–2950.
- Dubois, M., Gilles, K.A., Hamilton, J.K., Rebers, P.A., Smith, F., 1956. Colorimetric method for the determination of sugars and related substances. *Anal. Chem.* 28, 350–356.
- Ersahin, M.E., Ozgun, H., Lier, J.B.V., 2012. Effect of support material properties on dynamic membrane filtration performance. *Separ. Purif. Technol.* 48, 2263–2269.
- Frijns, J., Hofman, J., Nederlof, M., 2013. The potential of (waste)water as energy carrier. *Energy Convers. Manag.* 65, 357–363.
- Fuchs, W., Resch, C., Kernstock, M., Mayer, M., Schoeberl, P., Braun, R., 2005. Influence of operational conditions on the performance of a mesh filter activated sludge process. *Water Res.* 39, 803–810.
- Gao, T.Y., Gu, G.W., Zhou, Q., 2007. *Water Pollution Control Engineering*, third ed. Higher Education Press, Beijing.
- Gong, H., Wang, X., Zheng, M., Jin, Z., Wang, K., 2014. Direct sewage filtration for concentration of organic matters by dynamic membrane. *Water Sci. Technol.* 70, 1434–1440.
- Gong, H., Wang, Z.J., Zhang, X., Jin, Z.Y., Wang, C.P., Zhang, L.P., Wang, K.J., 2017. Organic and nitrogen recovery from sewage via membrane-based pre-concentration combined with ion exchange process. *Chem. Eng. J.* 311, 13–19.
- Guellil, A., Thomas, F., Block, J.C., Bersillon, J.L., Ginestet, P., 2001. Transfer of organic matter between wastewater and activated sludge flocs. *Water Res.* 35, 143–150.
- Hu, Y., Wang, X.C., Sun, Q., Ngo, H.H., Yu, Z., Tang, J., Zhang, Q., 2017. Characterization of a hybrid powdered activated carbon-dynamic membrane bioreactor (PAC-DMBR) process with high flux by gravity flow: operational performance and sludge properties. *Bioresour. Technol.* 223, 65–73.
- Kartal, B., Kuenen, J.G., Loosdrecht, M.C.M.V., 2010. Sewage treatment with anammox. *Science* 328, 702–703.
- Kiso, Y., Jung, Y.J., Ichinari, T., Park, M., Kitao, T., Nishimura, K., Min, K.S., 2000. Wastewater treatment performance of a filtration bio-reactor equipped with a mesh as a filter material. *Water Res.* 34, 4143–4150.
- Lee, W., Kang, S., Shin, H., 2003. Sludge characteristics and their contribution to microfiltration in submerged membrane bioreactors. *J. Membr. Sci.* 216, 217–227.
- Li, Z.H., Kuba, T., Kusuda, T., 2006. The influence of starvation phase on the properties and the development of aerobic granules. *Enzym. Microb. Technol.* 38, 670–674.
- Lowry, O.H., Rosebrough, N.J., Farr, L.A., Randall, R.J., 1951. Protein measurement with the folin phenol reagent. *J. Biol. Chem.* 193, 265–275.
- Lutchmiah, K., Cornelissen, E.R., Harmsen, D.J., Post, J.W., Lampi, K., Ramaekers, H., Rietveld, L.C., Roest, K., 2011. Water recovery from sewage using forward osmosis. *Water Sci. Technol.* 64, 1443–1449.
- Lutchmiah, K., Lauber, L., Roest, K., Harmsen, D.J.H., Post, J.W., Rietveld, L.C., Lier, J.B.V., Cornelissen, E.R., 2014. Zwitterions as alternative draw solutions in forward osmosis for application in wastewater reclamation. *J. Membr. Sci.* 460, 82–90.
- Mccarty, P.L., Bae, J., Kim, J., 2011. Domestic wastewater treatment as a net energy producer—can this be achieved? *Environ. Sci. Technol.* 45 (17), 7100–7106.
- Ren, X., Shon, H.K., Jang, N., Lee, Y.G., Bae, M., Lee, J., Cho, K., Kim, I.S., 2010. Novel membrane bioreactor (MBR) coupled with a nonwoven fabric filter for household wastewater treatment. *Water Res.* 44, 751–760.
- Sun, F.Y., Lv, X.M., Li, J., Peng, Z.Y., Li, P., Shao, M.F., 2014. Activated sludge filterability improvement by nitrifying bacteria abundance regulation in an adsorption membrane bioreactor (Ad-MBR). *Bioresour. Technol.* 170, 230–238.
- Vera, L., González, E., Díaz, O., Sánchez, R., Bohorque, R., Rodríguez-Sevilla, J., 2015. Fouling analysis of a tertiary submerged membrane bioreactor operated in dead-end mode at high-fluxes. *J. Membr. Sci.* 493, 8–18.
- Wang, X., Yuan, B., Chen, Y., Li, X., Ren, Y., 2014. Integration of micro-filtration into osmotic membrane bioreactors to prevent salinity build-up. *Bioresour. Technol.* 167, 116–123.
- Xiong, J., Fu, D., Singh, R.P., 2014. Self-adaptive dynamic membrane module with a high flux and stable operation for the municipal wastewater treatment. *J. Membr. Sci.* 471, 308–318.
- Yang, Z., Peng, X.F., Chen, M.Y., Lee, D.J., Lai, J.Y., 2007. Intra-layer flow in fouling layer on membranes. *J. Membr. Sci.* 287, 280–286.
- Yuan, B., Wang, X., Tang, C., Li, X., Yu, G., 2015. In situ observation of the growth of biofouling layer in osmotic membrane bioreactors by multiple fluorescence labeling and confocal laser scanning microscopy. *Water Res.* 75, 188–200.
- Yuan, D., Wang, Y., Qian, X., 2017. Variations of internal structure and moisture distribution in activated sludge with stratified extracellular polymeric substances extraction. *Int. Biodeterior. Biodegrad.* 116, 1–9.
- Yuan, M.C., Duujong, L., Yang, Z., Peng, X.F., Lai, J.Y., 2006. Fluorescent staining for study of extracellular polymeric substances in membrane biofouling layers. *Environ. Sci. Technol.* 40, 6642–6646.
- Zhang, J., Loong, W.L.C., Chou, S., Tang, C., Wang, R., Fane, A.G., 2012. Membrane biofouling and scaling in forward osmosis membrane bioreactor. *J. Membr. Sci.* 403–404, 8–14.
- Zhang, Q., Jie, Y.W., Loong, W.L.C., Zhang, J., Fane, A.G., Kjelleberg, S., Rice, S.A., McDougald, D., 2014. Characterization of biofouling in a lab-scale forward osmosis membrane bioreactor (FOMBR). *Water Res.* 58, 141–151.
- Zhang, X.Y., Wang, Z.W., Wu, Z.C., Lu, F.H., Tong, J., Zang, L.L., 2010. Formation of

- dynamic membrane in an anaerobic membrane bioreactor for municipal wastewater treatment. *Chem. Eng. J.* 165, 175–183.
- Zhou, X.H., Shi, H.C., Cai, Q., He, M., Wu, Y.X., 2008. Function of self-forming dynamic membrane and biokinetic parameters' determination by microelectrode. *Water Res.* 42, 2369–2376.
- Zou, L., Vidalis, I., Steele, D., Michelmore, A., Low, S.P., Verberk, J.Q.J.C., 2011. Surface hydrophilic modification of RO membranes by plasma polymerization for low organic fouling. *J. Membr. Sci.* 369, 420–428.